Journal of Surface Analysis Vol.15, No. 2 (2008) pp. 130−138
S. Hofmann Electron Backscattering in Sputter Depth Profiling Using AES, EPES, and REELS

Review

Electron Backscattering in Sputter Depth Profiling Using AES, EPES, and REELS

Siegfried Hofmann*
Max-Planck-Institute for Metals Research, Stuttgart, Germany
**s.hofmann@mf.mpg.de*

(Received: December 18, 2007; Accepted: March 3, 2008)

The main applications of electron backscattering in sputter depth profiling using AES and related electron spectroscopies such as elastic peak electron spectroscopy (EPES) and reflection electron energy loss spectroscopy (REELS) are briefly summarized. EPES depth profiling is particularly useful for improving the interfacial depth resolution in binary systems by selecting a suitable primary electron energy. With REELS depth profiling, the change of the IMFP during sputtering through an A/B interface can be quantitatively determined. Recently, a method for implementing the backscattering effect in the MRI model has been introduced and applied to AES depth profiles of single layer and multilayer structures. Its capability to provide quantification of measured profiles including the backscattering effect is outlined.

1. Introduction

Comparing the number of publication based on application of AES and XPS, it has become obvious that today XPS is preferred by the majority of researchers, although AES has a much better spatial resolution, a great advantage in the age of nanostructured materials. To the author's opinion, the main reasons for the more restricted usage of AES are the more complicated interpretation and quantification of AES, mainly caused by three basic differences: (i) the relatively complex Auger transition leads to complicated, multiline spectra, (ii) the secondary (and backscattered) electron background is much higher than in XPS and therefore leads to more difficult background subtraction problems (e.g. differentiation), and (iii) the signal intensity is not only proportional to the excitation intensity, as in XPS, but also to the intensity of backscattered electrons that are still capable of exciting Auger transitions in the acceptance area of the analyzer [1]. Last but not least, AES is traditionally done with a cylindrical mirror analyzer (CMA) that is more complicated to use in practice and has many shortcomings (such as a highly position sensitive energy and intensity and limited resolution) as compared to the concentric hemispherical analyzer (CHA). Therefore it was a pioneering step forward when Professor Keisuke Goto at the Nagoya Institute of Technology built the first metrological CMA [2], where many causes of measurement errors where minimized or avoided (such as stray electrons from the outer cylinder wall by applying soot, and excluding the energy dependence of detector sensitivity by employing a Faraday cup instead of the usual electron multiplier). Among many quantitative measurements in different fields, he measured quantitatively correct backscattered electron spectra that could be directly compared to theoretical calculations [3].

Backscattered electrons can be used in different ways. For example, in elastic peak electron spectroscopy (EPES), the peak intensity of elastically backscattered electrons gives information about the backscattering yield and therefore about the (average) atomic number and the inelastic mean free path (IMFP) of the sample [4]. By extending the spectral measurement to lower energies from the elastic peak, reflection electron energy loss spectroscopy (REELS) shows a structure that contains information about electronic losses such as plasmon excitation and therefore, can be used to reveal the dielectric function and the Inelastic Mean Free path (IMFP) of the electrons at the elastic peak energy [5]. Both methods can be successfully applied to depth profiling, as shown in sections 2.1. and 2.2.

From the beginning of AES applications, the backscattering effect was recognized and implemented in the basic equations of quantitative AES by a backscattering factor, $R_B = (1+r_B)$, by which the primary current has to be multiplied to yield the right magnitude responsible for the measured AES signal intensity. In this definition, the backscattering coefficient r_B characterizes the amount of intensity due to excitation by backscattered electrons. For more than 20 years, the well established Ichimura-Shimizu relations [6-8] have been used to derive r_B, which depends on the primary electron energy and incidence angle, on the Auger transition's ionization energy, and on the (average) atomic number of the elements. Recently, new calculations by Jablonski and Powell [9] and by Ding and coworkers [10] have shown that the Ichimura-Shimizu relations are only a rough approximation and can be at variance by up to 20 % from the new calculations. Furthermore, r_B additionally depends on the emission angle and can be even negative in case of very low energies and of very high (>80°) incidence angles. [10]. Although in the past the effect of backscattering was observed in the growth of thin layers [11] and several times in sputter depth profiling at interfaces [12-15], a full and quantitative description of depth profiles including backscattering was only attained recently [16,17]. In sections 3.1 and 3.2, the quantification of backscattering in sputter depth profiling using AES is briefly reviewed.

2. Direct use of electron backscattering spectra in depth profiling

2.1. Depth profiling using elastic peak electron spectroscopy (EPES)

The backscattering cross section depends directly on the atomic number [4]. Taking - as a first order approximation - the intensity of the elastically backscattered primary energy peak as proportional to the composition in a binary system of elements A and B, this dependence can be used for the determination of a depth profile through A/B interfaces [18,19]. This approach opens a useful way to obtain a better depth resolution as compared to normal (medium or high energy) AES peak measurement. The main reason is that in the quantitative profile description with MRI-model [20-22], out of the three MRI parameters-mixing length w (M), roughness σ ® and information depth (I) (as usually based on the electron escape depth λ), λ can be chosen almost freely by selecting a specific primary energy, in contrast to the fixed Auger energy. In EPES depth profiling, the effective electron escape depth, λ_{eff}, is composed of both the escape depth of the incoming primary electrons characterized by λ_{in}, and of and the escape depth of the emitted electrons, λ_{out}, both for the primary beam energy $E_{p.}$ Multiplying the respective exponential decay functions gives [19]:

$$\exp\left(-\frac{z-z_1}{\lambda_{eff}}\right)=\exp\left(-\frac{z-z_1}{\lambda_{in}}\right)\exp\left(-\frac{z-z_1}{\lambda_{out}}\right) \qquad (1a)$$

with

$$\lambda_{eff}=1/\left(1/\lambda_{in}+1/\lambda_{out}\right) \qquad (1b)$$

Note that for different incidence and emission angle, φ, the escape depth is different even for the same energy (= equal attenuation length λ^0), because $\lambda_{in} = \lambda^0 \cos \varphi_{in}$ and $\lambda_{out} = \lambda^0 \cos \varphi_{out}$. The value for λ^0 can be taken from the NIST tables of the attenuation length [23].

An example of the depth resolution improvement by Eq. (1b) is shown in Figs 1(a) and (b) [19]. For the experimental sputtering conditions: 1.5 keV Ar^+ ions, 74° incidence angle, the normalized Ge LMM (1145 eV) peak intensity is shown in Fig. 1(a) as a function of sputtering time and sputtered depth, together with the MRI fitting calculation [19]. Fitting was done with the following parameters: mixing length w = 1.7 nm, roughness parameter, σ = 0.8 nm, and information depth (taken here as electron escape depth), λ = 1.6 nm (with φ = 42°). An optimized fit reconstructed the (most simple) in depth distribution that is also displayed in Fig. 1. It shows a reduced Ge layer concentration (atomic fraction) of X/X_0 = 0.6 for layers 1 and 3 and X/X_0 = 0.37) for layer 2 [19]. Note that for AES, we can neglect λ_{in} in Eq. (1b), because for the primary energy 10 keV in Si (with λ_0 = 2.2 nm at 1147 eV)[23], λ_{in} = 10.1 nm >>λ_{out}. Therefore, for the AES profile, only λ_{out} (λ = 1.6 nm) is considered.

Figure 1(b) shows the elastic peak intensity at a peak energy of E_P= 1000 eV as a function of the sputtering time. It is obvious that Ge (Z=32) has a higher elastic reflection cross section as compared to Si (Z=14) [4]. Indeed Fig. 1(b) is rather similar to the Ge LMM profile in Fig1a, but the depth resolution of the EPES profile is obviously higher, in spite of the approximately equal

kinetic energy of the detected elastic peak (1000 eV) electrons as compared to the Ge (1147 eV) electrons. Evaluation of the EPES profile with the MRI model shows the parameters w = 1.7 nm (of course this has to be the same as in Fig. 1 because of the same sputtering conditions), σ = 0.8 nm, (σ = 0.6 nm seems to give a somewhat better fit, see Fig. 1(b)), and $\lambda = \lambda_{eff}$ = 0.8 nm. It follows that the effective escape depth change is responsible for the improved depth resolution in EPES depth profiling. According to Eqs. (1a) and (1b), the effective escape depth of 0.8 nm can be explained as follows:

For the primary beam with E_P = 1.0 keV, φ_{in} = 0 and the attenuation length λ^0_{in}(1147 eV) = 2.2 nm at 1147 eV we obtain λ^0_{in}(1000 eV)= λ_{in} = 2.0 nm, and $\lambda_{out} = \lambda^0_{in}$ cos 42.3 = 1.45 nm [19]. According to Eq. (1b), λ_{in} = 2.0 nm and λ_{out} = 1.45 nm combine to λ_{eff} = 0.84 nm**.** This value is in good agreement with the MRI best fit value of λ =

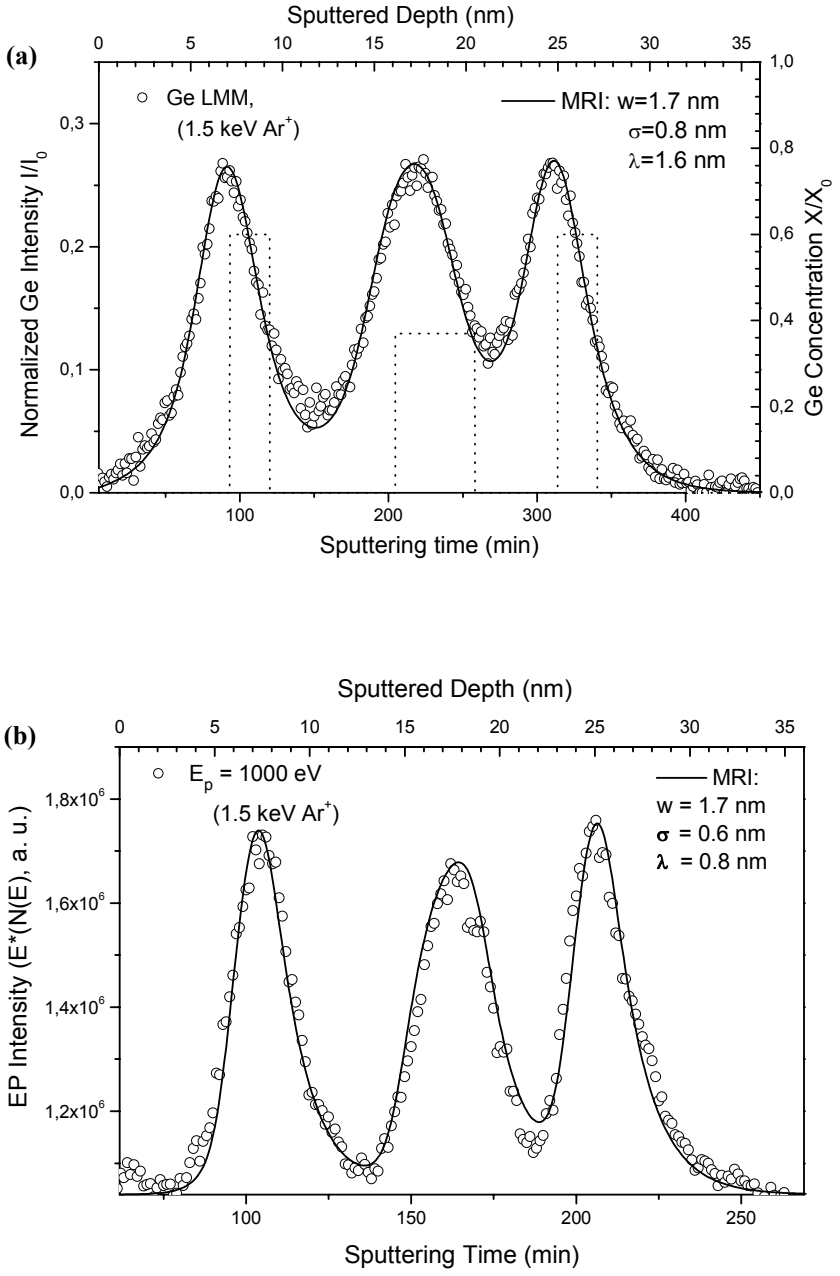

Fig. 1. AES Sputter depth profile of a Ge nanostructure (1-4-1 nm, 0.6-0.4-0.6 at%Ge) (open circles: measured data, line: MRI quantification for layer structure shown in upper picture as dotted line. MRI parameters see inset. (a) Measurement using the Ge (1147 eV) peak. (b) Measurement using EPES peak at E_p= 1000 eV. From Ref. [19].

0.8 nm (see inset in Fig 1(b)). In summary, comparison of EPES with AES depth profiling shows that the depth resolution function can be considerably improved in EPES depth profiling by reducing the effective electron escape depth. A further advantage is the much better signal-to-noise figure of the elastic peak, whereas a disadvantage is the limitation to strictly binary systems [19].

2.2. Application of reflection electron energy loss spectroscopy (REELS) to sputter depth profiling

REELS has been shown to be a powerful means to reveal the dielectric loss function and therefore to predict the inelastic mean free path (IMFP), from which the attenuation length (AL) can be calculated [5]. When sputtering through an A/B interface, it is obvious that the IMFP and the AL will gradually change from the value in A to that of the value in B. It is possible to directly follow this change by evaluation of REELS spectra taken during sputtering, as shown by Prieto *et al.* [24] for sputtering through the interface of a thin film of Fe on a Si substrate. At first, a quantitative analysis of REELS spectra after Yubero *et al.*[5] was used to calculate the electron loss function of pure Si and Fe, and then these results were used to determine the IMFPs in the electron energy range 250–2000 eV. These values are in good agreement with predictions from TPP-2M and with measured EPES values. The above method for pure Fe and Si was used to determine the variation of the IMFP at the Fe/Si interface when it is sputter depth profiled with 3 keV Ar^+ ions.

Figure 2(a) shows the variation of REELS spectra when sputtering through the Fe/Si interface [24]. In Fig. 2(b) the quantified change of the two components is plotted against the sputtering time for the primary energies E_p=500 and 1500 eV. From the energy dependence, the IMFPs for Si (1620 eV) and Fe (703 eV) are extrapolated and their variation as a function of the atomic percentage of the Fe component in the profile is depicted in Fig. 2(c)**.** The IMFP is observed to vary linearly with the Fe content in the altered layer at the interface which is generated by atomic mixing during sputtering. Despite the possibility of ion bombardment induced iron silicide formation, no indication of such an effect, e.g. a deviation from linearity, could be found in the REELS spectra (Figs. 2(a) and (b)) and in the result of IMFP values in Fig. 2c within the experimental error of the acquired data.

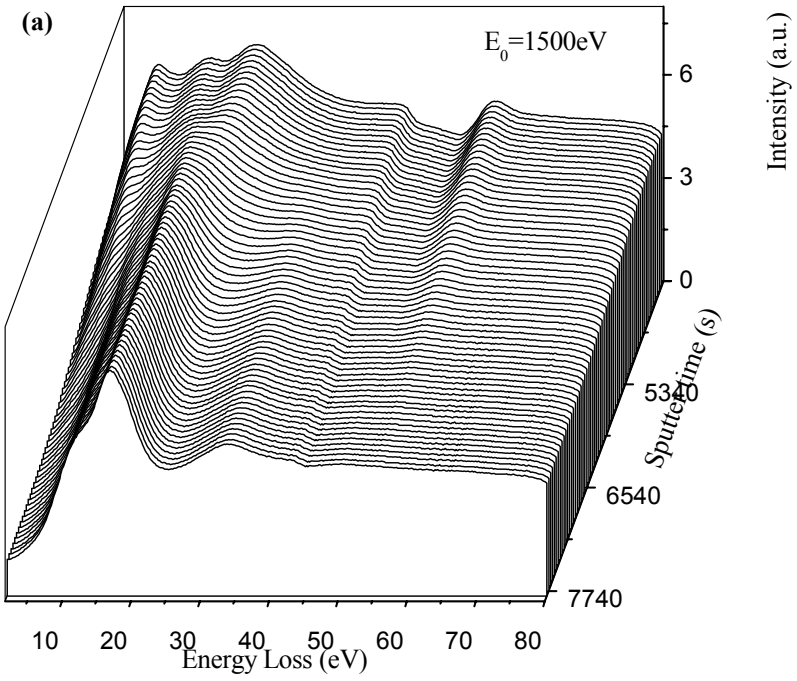

Fig. 2. (a) REELS spectra as a function of the sputtering time during sputtering through an Fe/Si interface, showing the gradual transition from pure Fe (front) to pure Si (back). The sample consists of a 150 nm thick Fe film deposited on a Si substrate which was carefully sputter cleaned before deposition. From Ref. [24].

In principle, the REELS profiling method can be applied to obtain the IMFP of compounds. Quantitative IMFP values and their change with composition of the altered layer can be used for an improved quantification of depth profiles at an interface using the MRI model [22].

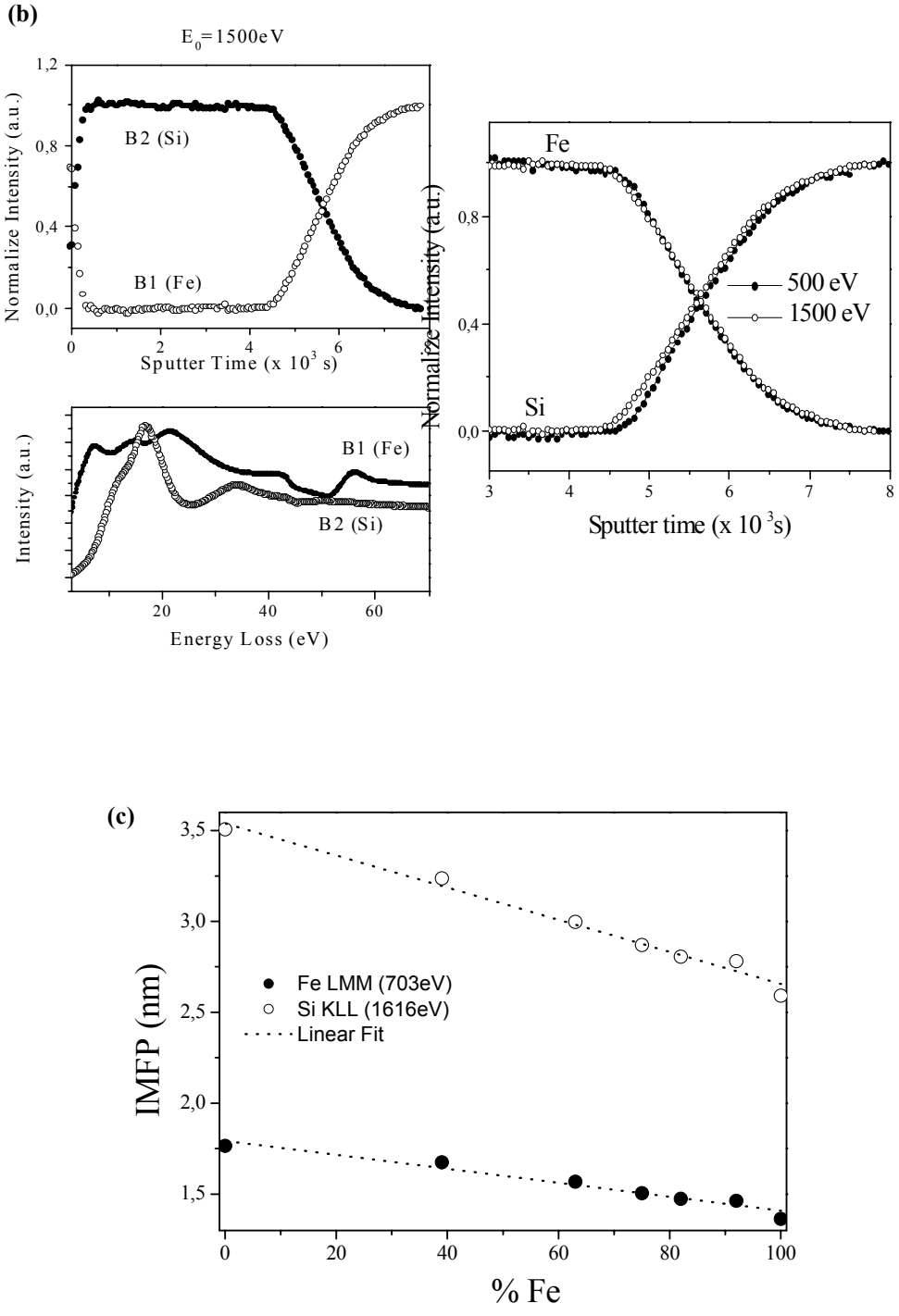

Fig. 2. (b) REELS sputter depth profile of a Fe/Si interface. Depth profiling was done with 3 keV Ar^+ ions. Left side lower picture shows REELS spectra of pure Fe (B1) and pure Si (B2), upper picture shows profile of these two components for E_p = 1500 eV and right picture for both E_p = 500 and 1500 eV. From Ref. [24]. (c) Variation of the inelastic mean free path (IMFP) of Si (1620 eV) and Fe (703 eV) as a function of the Fe content in the interface profile, derived from measurements in Figs. 2(a) and (b). From Ref. [24].

3. Effect of electron backscattering on Auger intensities in depth profiling

3.1. General observations and basic considerations

There are several published observations of the dependence of the Auger signal intensity of a thin film on the surface on its thickness, e.g. during evaporation of a film [11] or in sputter depth profiling of a thin layer [12-15] In these cases, quantification is more complicated because of the peculiar profile shape developing near the interface with sputtering time or depth. For example, if we consider the most simple case of sputtering through an interface between two elements A/B, where $r_B(B)>>r_B(A)$, a typical intensity increase of element A is obtained just before reaching the interface [12-15]. A similar effect is observed in reverse direction by evaporation of a layer of A on B and monitoring the layer growth with AES [11,25]. While Ichimura *et al.* [8] used Monte Carlo calculations to determine the backscattering correction factor for different film thicknesses and compared their data to the experimental data of a sputter depth profile of Si on W measured by Sato *et al.* [12], Barkshire *et al.* [26] proposed an analytical expression for the backscattering in layer-by-layer profiling based on a rather complicated relation given by Niedrig [27]. Using the expression of Barkshire *et al.* [26], Zalar *et al.* [15] first calculated the "ideal" profile expectation assuming ideally smooth, continuous thickness reduction, and then applied the MRI model to this calculated profile to obtain the measured one. This two- step procedure is cumbersome, particularly when taking into account that several calculations are necessary to obtain the optimum MRI fit. Because, in addition, the Niedrig-Barkshire equations are rather complicated and contain a number of new parameters, Hofmann and Wang [16] proposed a simple, semi-empirical expression for the depth dependent intensity that can directly be implemented in the MRI model. This expression is based on the ratio of the backscattering factors of components A and B, usually taken from the Ichimura-Shimizu relations [6-8], and on an exponential function with a "mean effective backscattering decay length" (MEBDL) as an adjustable parameter within certain limits. This basic functional dependence, already proposed in 1979 [25], is implemented in the MRI model as a factor before the term of the measured intensity. Several examples show that by using the modified MRI model, the measured AES depth profile can be calculated with a sufficient accuracy of typically less than a few percent. For the basic formalism of the MRI model, the reader is referred to refs. [20-22].

3.2. New developments: Quantification of the electron backscattering effect on the AES intensity using the MRI model

Quantification of sputter depth profiles obtained with AES for layers with markedly different backscattering factors from the substrate are increasingly influenced by the backscattered electrons from the latter with decreasing distance between the actual surface and the substrate. To describe this dependence, a new parameter, the "mean electron backscattering decay length" (MEBDL) $L_{B,A;A}$, was introduced [16,17], where A is the thin film element and B is the substrate. Thus, $L_{B,A;A}$ means the "MEBDL of (substrate) B on the AES intensity of element A in component A". Assuming for simplicity that the dependence with distance $z_0–z$ from the interface (at depth z_0) is exponential, the measured intensity, I_A, is given by

$$I_A = I_A(\mathrm{MRI}, R=1)R_{A,A} \times\left[1+\left(\frac{R_{B,A}}{R_{A,A}}-1\right)\exp\left(-\frac{z_0-z}{L_{B,A;A}}\right)\right] \quad (2)$$

where I_A(MRI,R=1) denotes the intensity calculated with the MRI model for backscattering factor R=1, $R_{A,A}$ and $R_{B,A}$ the backscattering factor of A for A and of B for A, respectively.

The results for two typical depth profiles, one for a carbon thin film on Ti, and the other for a gold thin film on a TiO_2/Capton substrate, are shown in Figs. 3(a) and (b). [16]. MRI parameters (w,σ,λ), backscattering factor ratios ($R_{B,A}/R_{A,A}$), and MEBDL values ($L_{B,A;A}$) are given in the insets. As seen from Eq. (2), the intensity is increasing for the ratio $R_{B,A}/R_{A,A}$ >1 (Fig. 3(a)), and decreasing for $R_{B,A}/R_{A,A}$<1 (Fig. 3(b)). Note that we have to use the MRI model modified by the sputtering rate ratio term, r(A,B). The reader is referred to Ref.[16,17] for more details and to Refs. [20-22] for basic information on the MRI model.

The above model description of a single layer on a substrate can easily be extended to the case of multilayers A/B/A/B…. by introducing an "effective backscattering factor" that depends on the layer thickness and of a more complicated definition of the MEBDL values, as in detail explained in ref. [17]. An example of a first application is shown in Figs. 4(a) and (b) for the AES sput-

ter depth profile of a Ni/C multilayer on an Si substrate consisting of five layers of Ni (38 nm thickness) and of five layers of C (25 nm thickness) [17]. Fig. 4(a) shows the measured profile of Ni together with the MRI calculation, and Fig. 4(b) shows the measured profile of C together with the MRI calculation, for optimized basic MRI and backscattering parameters ($R_{Ni,Ni}$, $R_{Ni,C}$, $R_{C,C}$, $R_{C,Ni}$, $R_{Si,C}$ and MEBDL values between 10 and 45 nm). It is interesting to note that the calculation correctly represents not only the shape of the individual profiles, but also the decrease in absolute intensity due to the diminishing backscattering effect in the vicinity of the Si substrate.

Perhaps the weakest point in the recent, altogether successful application of the incorporation of the backscattering effect in quantitative sputter depth profiling with the MRI model is the not well defined parameter "mean electron backscattering decay length" (MEBDL).

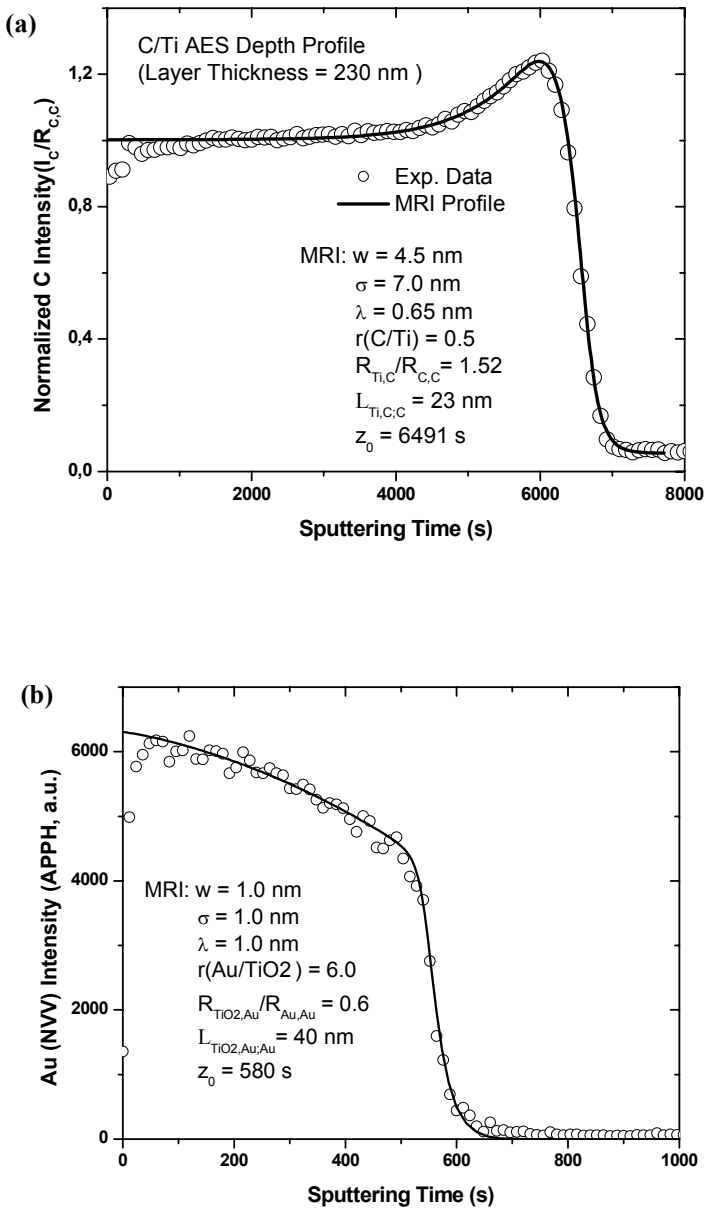

Fig. 3. (a) Depth profile (C 272 eV) of a 230 nm thick C layer on Ti. Open circles: measured points, line: MRI quantification (parameters see inset) with backscattering factor ratio R(Ti,C)/R(C,C) = 1.52. After Ref. [16], with measured data from Ref. [14]. (b) Au (68 eV) depth profile of a 80 nm au film on TiO_2/Kapton, with backscattering factor ratio $R(TiO_2,Au)/R(Au,Au)$ = 0.6. Open circles are measured data, full drawn line shows MRI quantification with the parameters given in the inset. From Ref. [16].

With respect to current theoretical understanding [9,10], it may looked upon as a rather strong simplification. However, the assumption of a MEBDL seems to work fairly well and its adjustment appears to be less critical than that of the backscattering factors. Necessary deviations of the latter from the Ichimura-Shimizu values may be not surprising in view of the new calculations of Jablonski and Powell [9] and of Ding *et al.* [10] including measurements of Goto [10] which show that deviations of up to 20% are to be expected.

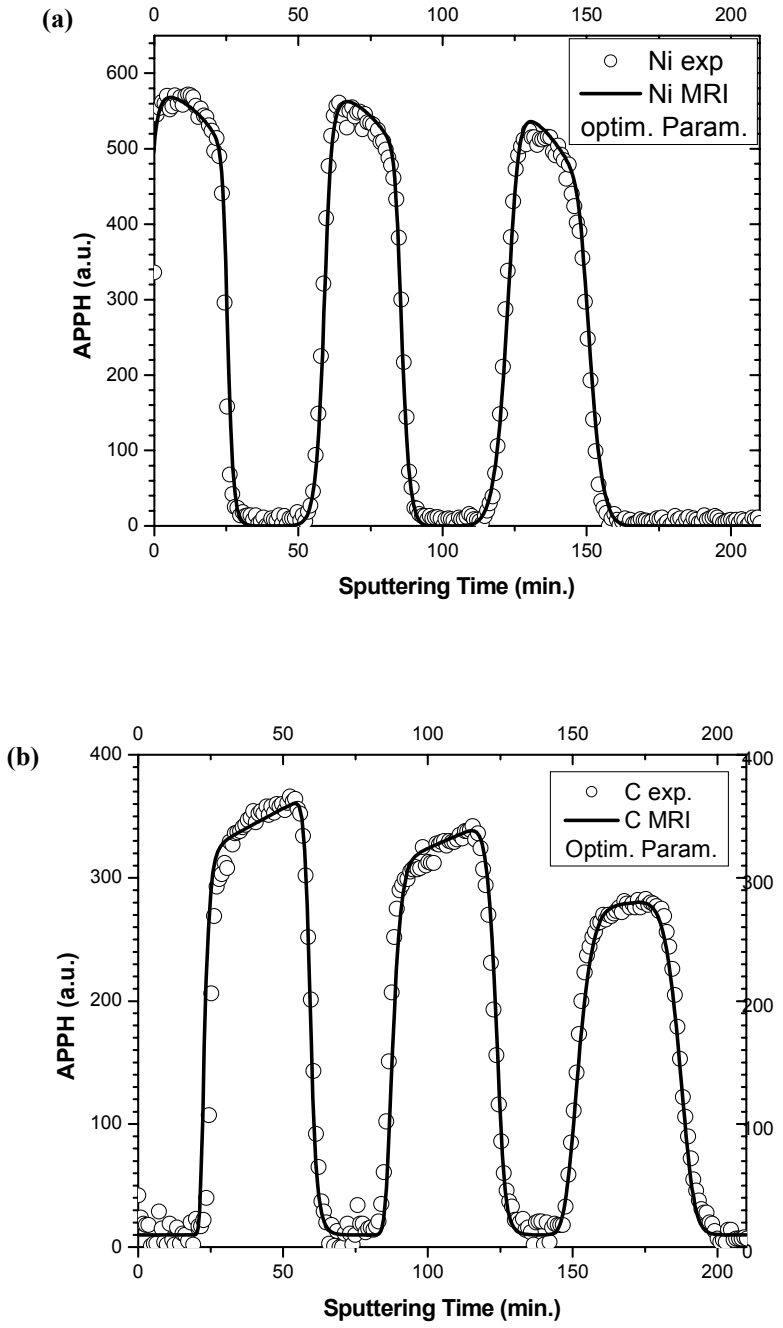

Fig. 4. (a) Ni sputter depth profile (848 eV Auger peak to peak heights, APPH) of a Ni/C (38/25 nm) multilayer. Open circles are measured points, solid line MRI quantification including effective backscattering factor correction. From Ref. [17], where details for the MRI calculation are given. (b) C sputter depth profile (272 eV Auger peak to peak heights, APPH) of a Ni/C (38/25 nm) multilayer. Open circles: measured points, solid line: MRI quantification including effective backscattering factor correction. From Ref. [17], where details for the MRI calculation are given.

4. Summary and conclusions

In this review, we have briefly considered the main applications of electron backscattering in sputter depth profiling using AES and related electron spectroscopies such as elastic peak electron spectroscopy (EPES) and reflection electron energy loss spectroscopy (REELS). Whereas the latter techniques are particularly useful for obtaining depth profiles with improved depth resolution and for obtaining the change of the IMFP when sputtering through an A/B interface, the recently proposed methods for implementing the backscattering effect in the MRI model applied to single layer [16] and to multilayer depth profiles with AES [17] have shown a satisfactory quantitative representation of measured profiles. The next step will be an extension to general multielemental depth profiles which is in progress.

5. References

[1] M. P. Seah, chap. 5 in *Practical Surface Analysis*, 2nd ed., D. Briggs and M.P. Seah, eds, Vol.1: AES and XPS, Wiley, Chichester (1990), pp. 203, 206 and 251.

[2] K. Goto, N. Sakibara, Y. Takeichi, Y. Numata, and Y. Sakai, Surf. Interface Anal. **22**, 75 (1994).

[3] Z.J. Ding, H. M. Li, K. Goto, Y. Z. Yang, and R. Shimizu, *J. Appl. Phys.* **96**, 4598 (2004).

[4] G. Gergely, *Surf. Interface Anal.* **3**, 201 (1981).

[5] F. Yubero, S. Tougaard, E. Elizalde, and J. M. Sanz, *Surf. Interface Anal.* **20**, 719 (1993).

[6] S. Ichimura and R. Shimizu, *Surf. Sci.* **112**, 386 (1981).

[7] R. Shimizu, *Jpn. J. Appl. Phys.* **22**, 1631 (1983).

[8] S. Ichimura, Ding-Ze Jun, and R. Shimizu, *Surf. Interface Anal.* **13**, 149 (1988).

[9] A. Jablonski and C. J. Powell, *Surf. Sci.* **574**, 219 (2005).

[10] Z. J. Ding, W. S. Tan, and Y. G. Li, *J. Appl. Phys.* **99**, 084903 (2006).

[11] M. L. Tarng and G. K. Wehner, *J. Appl. Phys.* **44**, 1534 (1973).

[12] L. Meda and G. Queirolo, *Surf. Sci.* **147**, 576 (1984).

[13] T. Sato, Y. Nagasawa, T. Sekine, Y. Sakai, and D. Buonaquisti, *Surf. Interface Anal.* **14**, 787 (1989).

[14] H. C. Swart, A. J. Jonker, C. H. Claassens, R. Chen, L. A. Venter, P. Ramoshebe, E. Wurth, J. J. Terblans, and W. D. Roos, *Appl. Surf. Sci.* **205**, 231 (2003).

[15] A. Zalar, J. Kovač, B. Praček, S. Hofmann, and P.Panjan, *Appl. Surf. Sci.* **252**, 2056 (2005).

[16] S. Hofmann and J. Y. Wang, *Surf. Interface Anal.* **39** 324 (2007).

[17] S. Hofmann, J. Y. Wang and A. Zalar, *Surf. Interface Anal.* **39** 787 (2007).

[18] A.Konkol and M.Menyhard, *Surf. Interface Anal.* **25**, 699 (1997)

[19] V. Kesler and S. Hofmann, *Surf. Interface Anal* **33**, 635 (2002).

[20] S. Hofmann, *Surf. Interface Anal.* **35**, 556 (2003).

[21] S. Hofmann, *Appl. Surf. Sci.* **241** 113 (2005).

[22] S. Hofmann and J. Y. Wang, *J. Surf. Anal.* **13**, 142 (2006).

[23] C. J. Powell and A. Jablonski, *NIST Electron Effective-Attenuation-Length Database*, ver. 1.0 (SRD 82). US Dept. of Commerce, National Institute of Standards and Technology, Gaithersburg (2001).

[24] P. Prieto, S.Hofmann, E. Elizalde, and J.M. Sanz, *Surf. Interface Anal.* **36**, 1392 (2004).

[25] S. Hofmann, *Mikrochim. Acta Suppl.* **8**, 71 (1979).

[26] I.R. Barkshire, M. Prutton, and D. K. Skinner, *Surf. Interface Anal.* **17**, 213 (1991).

[27] H. Niedrig, in: *Electron Beam Interactions with Solids*, p. 51, SEM Inc. AMF O'Hare, Chicago 1983.